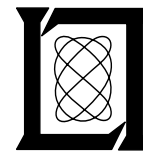# Multifunction Phased Array Radar Pulse Compression Limits

J.Y.N. Cho

25 April 2006

Lincoln Laboratory

MASSACHUSETTS INSTITUTE OF TECHNOLOGY

LEXINGTON, MASSACHUSETTS

1. Report No. ATC-327	2. Government Accession No.	3. Recipient's Catalog No.	
4. Title and Subtitle **Multifunction Phased Array Radar Pulse Compression Limits**		5. Report Date **25 April 2006**	
		6. Performing Organization Code	
7. Author(s) John Y.N. Cho		8. Performing Organization Report No. **ATC-327**	
9. Performing Organization Name and Address **MIT Lincoln Laboratory** **244 Wood Street** **Lexington, MA 02420-9108**		10. Work Unit No. (TRAIS)	
		11. Contract or Grant No. **FA8721-05-C-0002**	
12. Sponsoring Agency Name and Address **Department of Transportation** **Federal Aviation Administration** **800 Independence Ave., S.W.** **Washington, DC 20591**		13. Type of Report and Period Covered **Project Report**	
		14. Sponsoring Agency Code	

15. Supplementary Notes
This report is based on studies performed at Lincoln Laboratory, a center for research operated by Massachusetts Institute of Technology, under Air Force Contract FA8721-05-C-0002.

16. Abstract

An active phased array radar with distributed low-peak-power transmit modules requires pulse compression to provide high sensitivity and fine range resolution. A long transmitted pulse, however, has accompanying problems such as a near-range blind zone for the transmitting channel and loss of other gate data (dead gates) in other channels for a multichannel system. In this report the trade-off between the benefits and costs of pulse compression (lengthening) for multifunction phased array radars (MPARs) are analyzed. Specific results are presented for a three-channel MPAR and a two-channel terminal-area MPAR (TMPAR) that have been proposed as replacement systems for current U.S. civil-sector aircraft and weather surveillance radar systems. The recommended maximum compression ratio is 130 for the MPAR and 80 for the TMPAR. The results are independent of radar peak power and antenna gain, and represent upper bounds. Actual pulse compression ratios that would be employed are likely to be somewhat less than these values, based on fulfilling specific sensitivity and scan-time requirements with specific radar physical parameters.

17. Key Words	18. Distribution Statement		
multifunction phased array radar, pulse compression, dead gates, blind zone	This document is available to the public through the National Technical Information Service, Springfield, VA 22161.		

19. Security Classif. (of this report) Unclassified	20. Security Classif. (of this page) Unclassified	21. No. of Pages 35	22. Price

FORM DOT F 1700.7 (8-72)   Reproduction of completed page authorized

ABSTRACT

An active phased array radar with distributed low-peak-power transmit modules requires pulse compression to provide high sensitivity and fine range resolution. A long transmitted pulse, however, has accompanying problems such as a near-range blind zone for the transmitting channel and loss of other gate data (dead gates) in other channels for a multichannel system. In this report the trade-off between the benefits and costs of pulse compression (lengthening) for multifunction phased array radars (MPARs) are analyzed. Specific results are presented for a three-channel MPAR and a two-channel terminal-area MPAR (TMPAR) that have been proposed as replacement systems for current U.S. civil-sector aircraft and weather surveillance radar systems. The recommended maximum compression ratio is 130 for the MPAR and 80 for the TMPAR. The results are independent of radar peak power and antenna gain, and represent upper bounds. Actual pulse compression ratios that would be employed are likely to be somewhat less than these values, based on fulfilling specific sensitivity and scan-time requirements with specific radar physical parameters.

TABLE OF CONTENTS

Page

LIST OF ILLUSTRATIONS

LIST OF TABLES

1. INTRODUCTION

Currently in U.S. civilian airspace, weather and aircraft surveillance by ground-based radars are conducted through four separate networks. Each of these government operated networks has its own primary mission and is composed of different types of radars (Airport Surveillance Radars (ASRs), Air Route Surveillance Radars (ARSRs), Next Generation Weather Radar (NEXRAD), and Terminal Doppler Weather Radar (TDWR). Most of these systems are mechanically scanned with a limited capacity for carrying out multiple missions. They also incur increasing maintenance costs with age. The various agencies responsible for these radars plan to extend their lifetimes until about 2020. After that time, there are presently no concrete plans for procuring replacement radars for the networks.

An alternative to replacing the radars for the different networks with correspondingly different radars is to design a multifunction phased array radar (MPAR), sited appropriately across a single replacement network, that would fulfill all the surveillance requirements currently provided by the four separate radar networks. This option was proposed and studied [1], with the conclusion that the 513 radars comprising today's networks could effectively be replaced by 145 full-size MPARs and 144 scaled-down terminal-area MPARs (TMPARs). If the cost of the MPAR could be brought down to a reasonable level, then lower maintenance costs and the elimination of infrastructural and administrative redundancy may result in dramatic long-term cost savings as well as improved data quality and increased network flexibility for other applications such as homeland defense.

There are many technical challenges, however, to making such an MPAR a reality. Many of these issues are discussed in [1]. One of the fundamental issues is being able to meet the volume scan update rate requirements for all four surveillance functions corresponding to the four radar networks. These are approximately 5 s (terminal aircraft), 12 s (en route aircraft), 60 s (terminal area weather), and 300 s (regional weather). In order to meet these time constraints and provide optimal surveillance performance for each mission, it is necessary to operate the MPAR simultaneously on multiple frequency channels. By collapsing the two weather surveillance functions into one channel, the MPAR would then transmit and receive on three frequency channels. The TMPAR would only require two channels (terminal aircraft and terminal weather).

In moving from traditional radars with a single-source, high-peak-power transmitter to a modern active array with distributed low-peak-power transmit/receive (TR) modules, one must usually resort to pulse compression techniques in order to maintain range resolution and sensitivity. Since the MPAR and TMPAR must be affordable, and the TR module cost is nonlinearly dependent on its output power, high-power TR modules are not considered to be a viable option at this time.

Lengthening the transmitted pulse, however, creates its own problems. First, the nearby range corresponding to the pulse length becomes a blind zone, because reception is not possible during transmission. This blind zone can be covered separately using a much shorter fill pulse as long as the reduced sensitivity still meets the surveillance requirements for those ranges. If the pulse compression ratio is made too large (blind zone too large), then the sensitivity with the fill pulse would not be able to

fulfill the surveillance requirements at the farthest reaches of the blind zone. This is a trade-off analysis that sets a limit on how much pulse compression (lengthening) can be used.

Another issue associated with lengthening the transmitted pulse in a multichannel system is that when one channel is transmitting, the other channels cannot be receiving due to cross-channel interference. This creates "dead" gates as illustrated in Figure 1. The loss of received data degrades detection performance and the discontinuity in the time series makes spectral processing more problematic. The balance between increased sensitivity and data loss also sets a limit on pulse length and may even provide an insight on the optimal pulse length for maximum detection performance. The subject of this report is the analysis of the blind-zone and pulse-data-loss trade-offs.
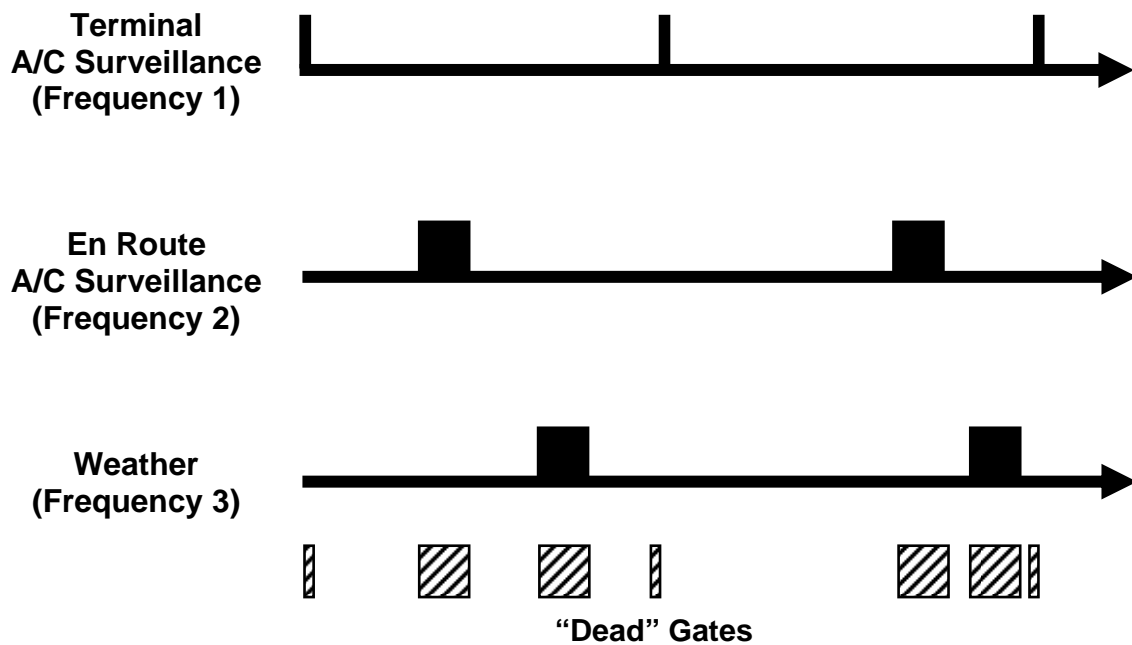

Figure 1. Example pulse scheduling for a three-channel MPAR.

2. BLIND ZONE

Let us begin by assuming that pulse compression ratio C is applied to increase the average power on target while maintaining the same range resolution as a simple pulse of length τ_0. The pulse width is increased to $C\tau_0$ and the length of the blind zone is $Cc\tau_0/2$, where c is the speed of light. Let us further assume that the simple pulse will be used as the fill pulse to cover the blind zone. Then if C is too big, the blind zone length will exceed the detection range for the simple pulse.

The detection range is proportional to $P^{1/m}$, where P is transmitted power, $m = 4$ for discrete targets such as aircraft, and $m = 2$ for volume-filling targets such as weather. (P can be replaced by C, assuming ideal pulse compression.) If the required detection range is exactly met by the long pulse with compression ratio C, then it is given by

$$R = R_0 C^{1/m} \, ,$$

(1)

where R_0 is the detection range of the simple pulse. (This expression ignores any dead gate/pulse overlap avoidance effects. Inclusion of such effects has a minimal impact on the results of this section, because the degradation of detection range for both the simple and long pulse tends to cancel each other.) Then, since the simple pulse detection range must be greater than or equal to the blind zone length, we get

$$R_0 \geq \frac{Cc\tau_0}{2} \, .$$

(2)

Substituting (1) into (2) we get

$$C \leq \left(\frac{2R}{c\tau_0} \right)^{\frac{m}{m+1}} .$$

(3)

The required range resolution of 150 m sets $\tau_0 = 1$ μs. For the TMPAR, the required range coverage of 60 nautical miles (111 km) yields maximum compression ratios of 200 (aircraft mode) and 80 (weather mode). For the MPAR, pulse compression is only applied to the weather and en route aircraft surveillance channels; the terminal aircraft surveillance channel will transmit a simple pulse and also be used as the fill pulse mode. In this case, the required detection range of 250 nautical miles (460 km) for the en route aircraft mode yields a maximum compression ratio of 620. To be conservative, for the weather channel we take the NEXRAD Doppler range coverage requirement of 230 km, which gives a maximum compression ratio of 130.

The above analysis works well for the aircraft surveillance mode, where detection range is well defined. For the weather mode, however, "detection" is not a simple binary decision, and, thus, "detection range" is not well defined. For terminal area surveillance, especially, the desired level of

3

sensitivity to weather targets is higher at close ranges, because the more critical areas, such as the airport, are usually closer to the radar. Therefore, equating the sensitivity at maximum range to the sensitivity required for the fill-pulse range may not be sufficient. Also the sensitivity discontinuity present at the fill-pulse-to-long-pulse crossover range could adversely affect automatic feature detectors, e.g., gust front and microburst recognition algorithms. Therefore, the maximum pulse compression to be used for the weather mode must be based on an analysis that includes these factors as well as further factors to be discussed in the following sections.

3. DEAD GATES AND PULSE OVERLAP AVOIDANCE

To keep things general, let each frequency channel have its own pulse length τ and average pulse-repetition interval (PRI) T. We say "average" because variable PRI transmission is useful for purposes such as blind speed avoidance for aircraft surveillance and range-velocity ambiguity mitigation for weather sensing. (Note that such asynchronous transmission would sometimes result in pulse overlap between channels without adaptive PRI adjustment in real time. This issue will be discussed later.) For a given channel k the fraction of gates lost due to transmission in all other channels is

$$L_k = \frac{T_k}{T_k - \tau_k} \sum_{l \neq k} \frac{\tau_l}{T_l} ,$$ (4)

where the summation is taken over all other channels. This expression reduces to

$$L = \tau \frac{N-1}{T-\tau}$$ (5)

for an N-channel system if τ and T are the same for all channels.

For the full-size three-channel MPAR, the nominal average PRIs that would be used in each channel are 1 ms (terminal aircraft), 3 ms (en route aircraft), and 1 ms (weather). To roughly match the sensitivity of the current radars, pulse compression is not needed for the terminal aircraft mode, but it is needed for the other two modes to roughly the same degree [1]. The required range resolution of 150 m sets the length of the terminal-aircraft-mode pulse to 1 µs. We can then express the pulse length of the other two modes as C x 1 µs, where C is the pulse compression ratio. Given these relationships (4) can be used to compute the fraction of dead gates as a function of C for the three channels:

$$L_{\text{Terminal}} = 1.335 \times 10^{-3} C ,$$ (6)

$$L_{\text{EnRoute}} = \frac{3C+3}{3000-C} , \text{ and}$$ (7)

$$L_{\text{Weather}} = \frac{C+3}{3(1000-C)} .$$ (8)

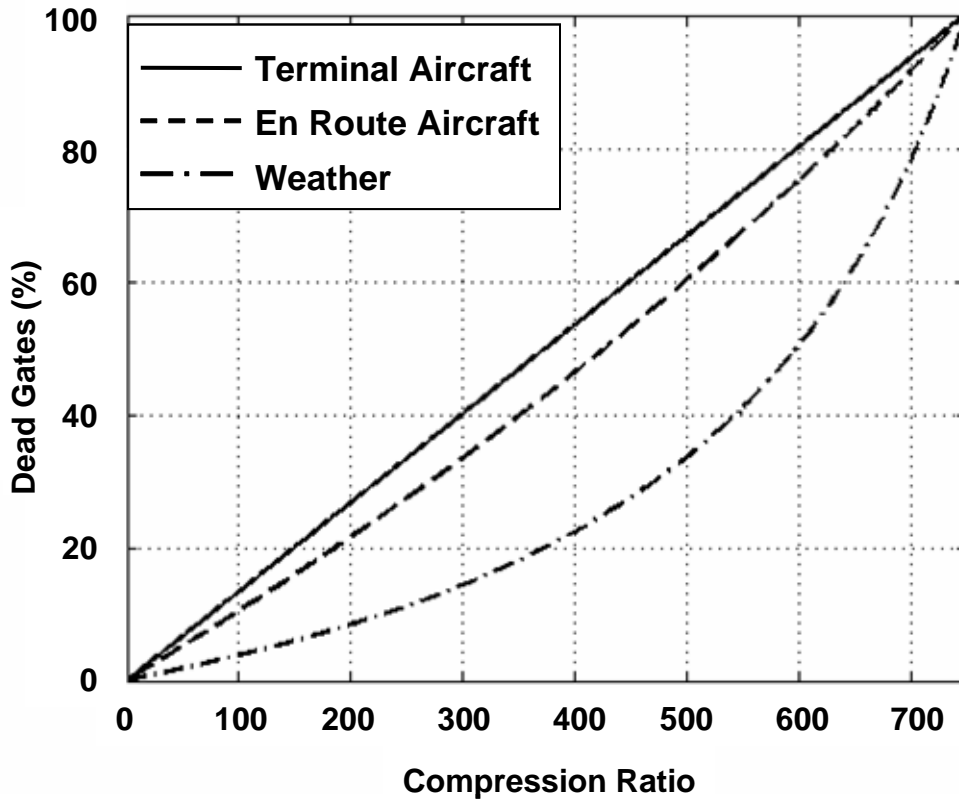Figure 2 shows a plot of these functions.

Figure 2. Percentage dead gates vs. pulse compression ratio for the full-scale three-channel MPAR.

For the TMPAR, we expect pulse compression to be needed for both surveillance modes to about the same degree to meet the sensitivity requirements. In this case, since the average PRIs for terminal-area aircraft and weather surveillance modes are the same, we can use (5) to compute the fraction of dead gates for both channels. The result is plotted in Figure 3 as a function of pulse length normalized to PRI, since τ and T are the same for both channels.

Earlier we alluded to the pulse overlap problem. When employing asynchronous transmission on multiple channels, there will be instances when more than one channel wants to be in the transmit mode at the same time. To avoid such coincidences one would need to have an adaptive pulse scheduler that would delay one of the potentially conflicting pulses, which would alter the PRI pattern for that channel.

Of course, changing the expected PRI pattern can then have negative consequences for Doppler filtering in aircraft surveillance mode and clutter filtering and Doppler moment estimation in weather surveillance mode. To simplify matters, let us study the worst-case scenario, where the pulse to be shifted is dropped and no data are recovered from it.
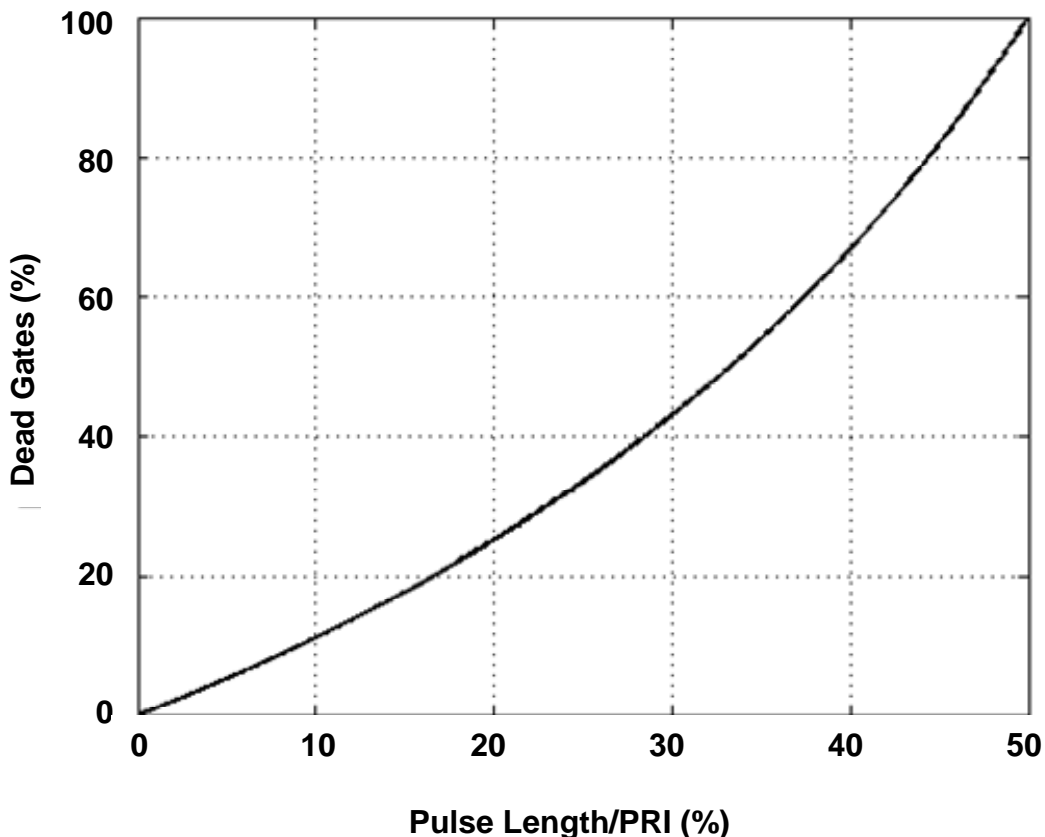

Figure 3. Percentage dead gate loss vs. pulse length normalized to PRI for the TMPAR.

First we wish to compute the probability of pulse overlap. This can be done through a computer simulation. Pulse overlap rates depend on the particular PRI patterns employed on each channel. For a realistic set of PRI sequences to be used in the three-channel MPAR, we select typical sets currently used in the ASR-9 for the terminal aircraft surveillance channel (block staggered: 10 x 824 μs, 8 x 1060 μs), the ARSR-4 for the en route aircraft surveillance channel (staggered: 2500, 2700, 2916, 3150, 3402, 3674, 3969, 4286, 4629 μs), and the NEXRAD (constant: 1000 μs) for the weather channel. For the two-channel TMPAR, the same sets for the terminal aircraft and weather surveillance channels are used. Then letting 1 μs be the increment, we step through in time and record each pulse overlap event. A two-pulse overlap counts as one event and a three-pulse overlap counts as two events, because those numbers correspond to the number of pulses that would have to be shifted or deleted. The pulse overlap rate is

then the number of events divided by the total number of pulses. The rates appeared to converge fairly well after about 5 million time increments. For the results to follow, we used 50 million time increments for each pulse overlap computation.

The results of pulse overlap rate vs. compression ratio are shown in Figure 4 for the MPAR and TMPAR cases. As in the dead-gate study, pulse compression is only applied in the weather and en route aircraft surveillance channels in the three-channel case, whereas it is applied to both aircraft and weather surveillance channels in the two-channel case. Note that our three-channel case has a lower overlap rate. This counterintuitive result is due to the long PRIs of the en route aircraft surveillance mode and the fixed 1-μs pulse length of the terminal aircraft surveillance mode of the three-channel case.
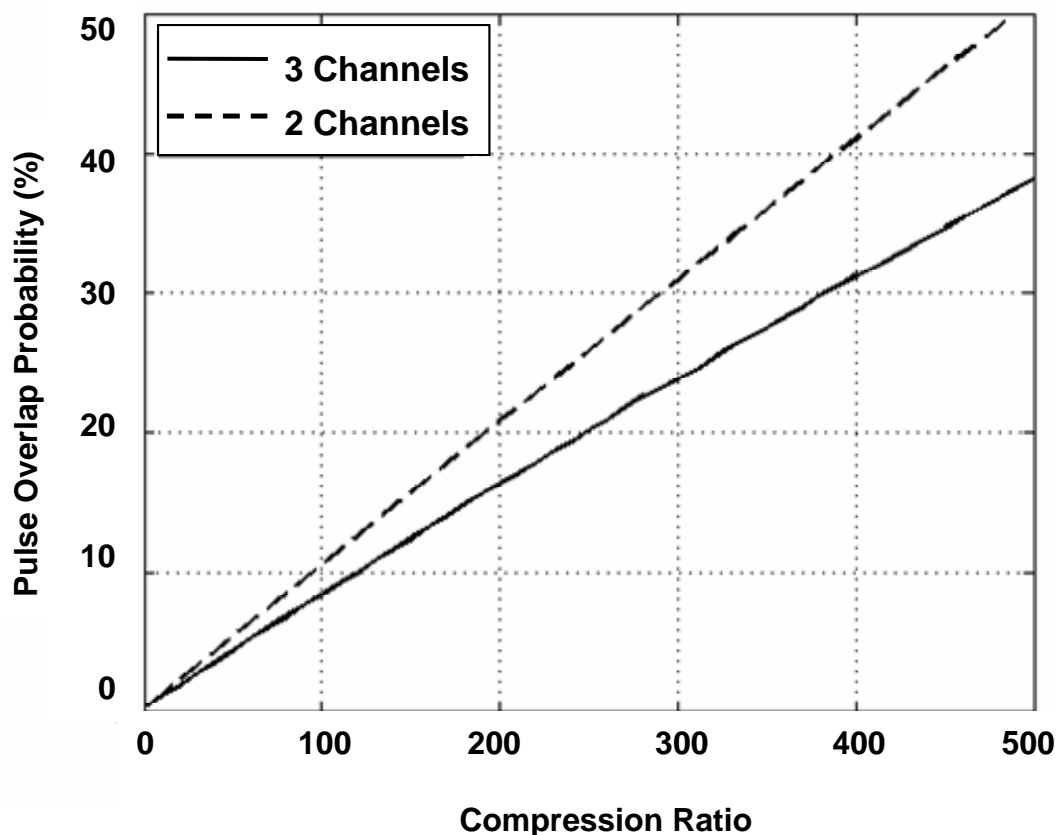

Figure 4. Probability of pulse overlap vs. pulse compression ratio for the MPAR and TMPAR.

For ease of use in further computations, we can fit polynomials to the curves of Figure 4. For the MPAR case, a second-degree polynomial with coefficients $a_2 = -1.38 \times 10^{-7}$, $a_1 = 8.26 \times 10^{-4}$, and $a_0 = 2.27 \times 10^{-3}$, where C is the independent variable, fit the data well. For the TMPAR case, a linear fit with coefficients $a_1 = 1.02 \times 10^{-3}$ and $a_0 = 2.58 \times 10^{-3}$ worked well.

8

We can now combine the data loss probability due to dead gates and pulse overlap avoidance. In order not to double count the loss from the two sources, the total pulse loss probability is expressed as

$$L_{\text{Total}} = L_{\text{DeadGates}} + (1 - L_{\text{DeadGates}})L_{\text{PulseOverlap}} \quad . \tag{9}$$

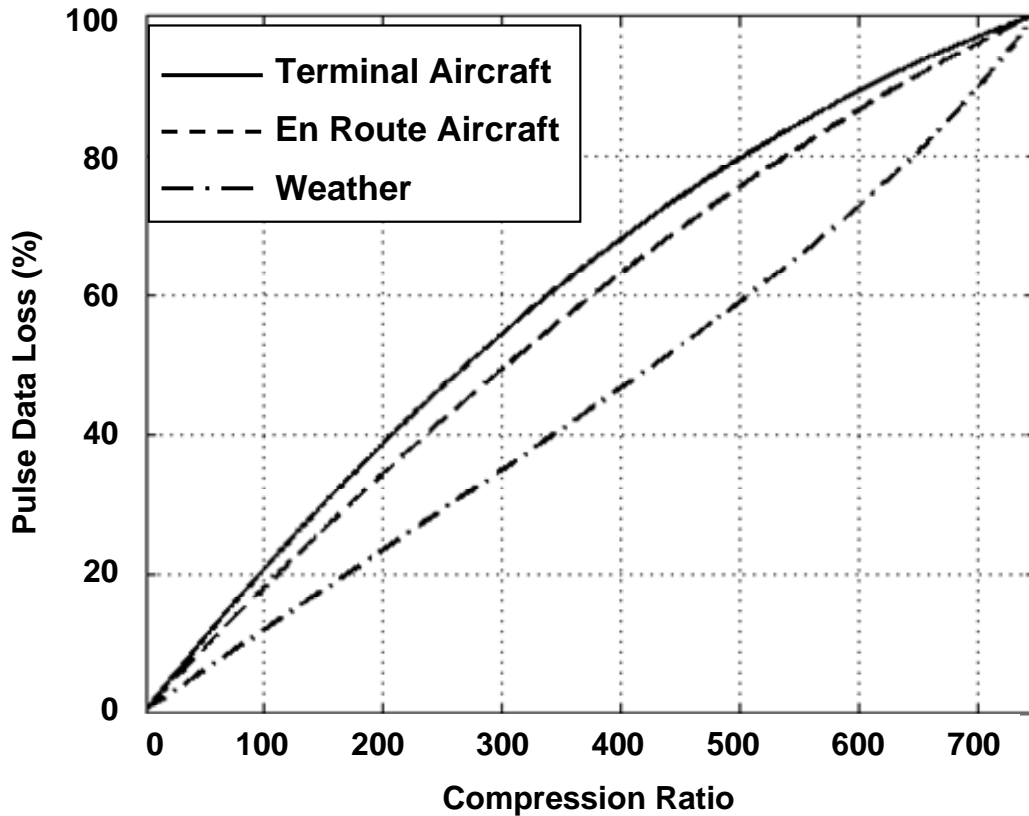The results are displayed in Figures 5 and 6.

Figure 5. Pulse data loss probability per channel due to dead gates and pulse overlap avoidance vs. pulse compression ratio for the MPAR.
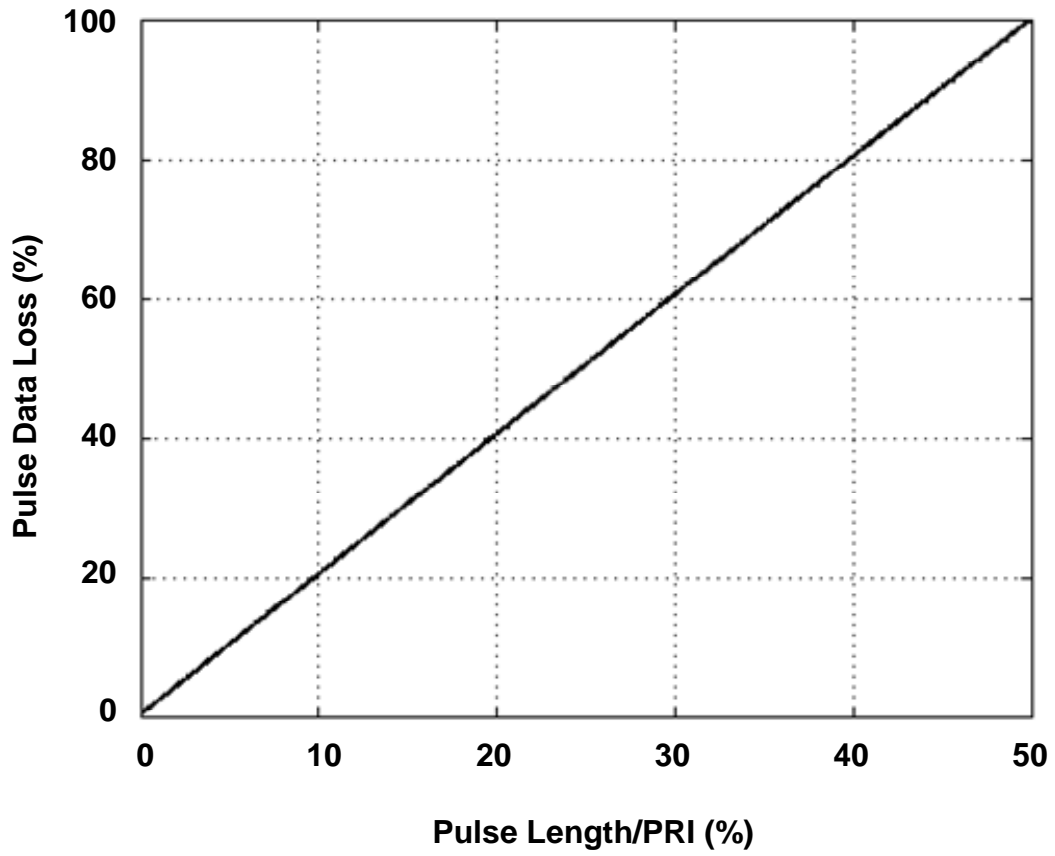
Figure 6. Pulse data loss probability per channel due to dead gates and pulse overlap avoidance vs. pulse length normalized to PRI for the TMPAR.

10

4. AIRCRAFT SURVEILLANCE MODE

Aircraft probability of detection (POD) by radar is improved by increasing the single-pulse signal-to-noise ratio (SNR), S, and the number of pulse returns integrated, n [2]. By increasing the pulse length (compression ratio) one increases the former but decreases the latter due to dead-gate and pulse-overlap-avoidance loss. Therefore, there must be a point at which increasing pulse length will be detrimental to aircraft POD.

To calculate the effect of pulse compression on aircraft POD, we use the analytic radar target detection equation given in [3]

$$P_d(S, P_{fa}, n, n_e) = 1 - \chi_c^2 \left[\frac{\chi_c^{-2}(1 - P_{fa}, 2n) - 2(n - n_e)}{\frac{n}{n_e} S + 1}, 2n_e \right] , \tag{10}$$

where χ_c^2 is the cumulative chi-square distribution function and χ_c^{-2} is its inverse, P_{fa} is the false alarm probability, and n_e is the number of independent Rayleigh-distributed signal samples observed, which is dependent on the target type. The four classical target types defined by Swerling [4] correspond to $n_e = 1$ (case 1), $n_e = n$ (case 2), $n_e = 2$ (case 3), and $n_e = 2n$ (case 4). The assumption for case 1 is that the echo pulses received from a target on any one scan are of constant amplitude throughout the entire scan, but are uncorrelated from scan to scan, and that the target consists of many independent scatterers of comparable cross sections. Case 1 puts more demand on the radar than do the other cases, and is the one most often assumed for a nonspecific fluctuating target. We will therefore choose case 1 for our study.

We now wish to compute P_d as a function of pulse length or compression ratio C. S is clearly proportional to C, while n decreases in proportion to L. We thus use (9) in (10) to get P_d, with $S = S_0 C$ and $n = n_0(1 - L)$, where S_0 and n_0 are initial values corresponding to no pulse compression ($\tau_0 = 1$ μs on all channels). $P_{fa} = 10^{-6}$ will be used for all cases. For the en route aircraft surveillance mode in the three-channel case, we assume $n_0 = 10$. The results are shown in Figure 7 for three cases of S_0. As expected, the benefit of boosting the SNR by increasing the pulse length is quickly exhausted if S_0 is high. Interestingly, however, the maximum POD is achieved at the same pulse compression ratio (390) for all cases of S_0.
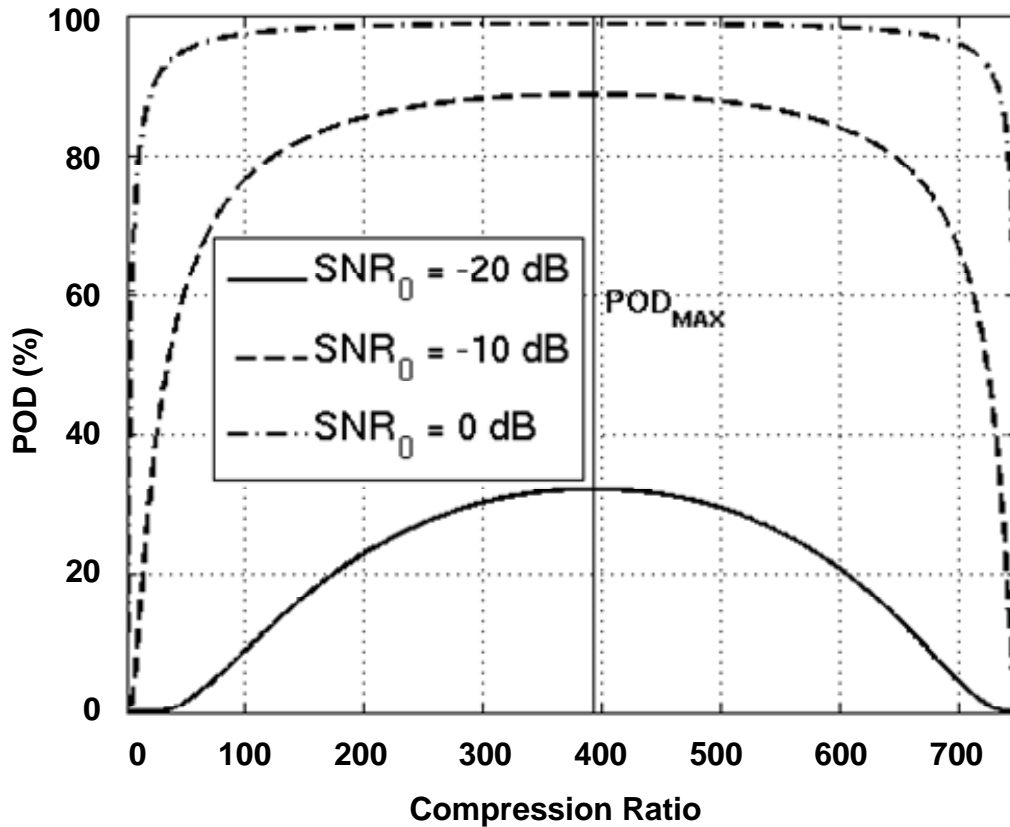
Figure 7. POD vs. pulse compression ratio for the en route aircraft surveillance mode of the full-scale three-channel MPAR.

The same calculations were performed for the terminal aircraft surveillance channel (Figure 8). In this case there is no POD maximum, because the pulse length is fixed in this channel. Increased pulse compression in the other channels only degrades the POD in this channel. Results for the aircraft channel of the TMPAR with $n_0 = 18$ are shown in Figure 9. Here the maximum POD occurred at $\tau/T = 29\%$ ($C = 290$).
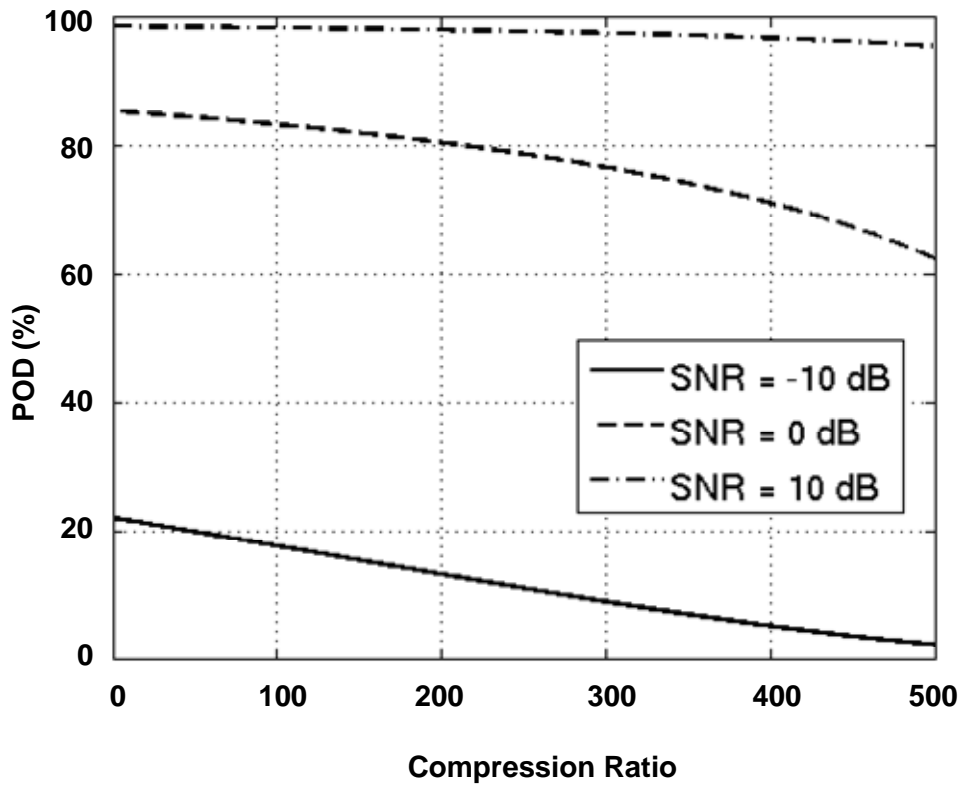
Figure 8. POD vs. pulse compression ratio for the terminal-area aircraft surveillance mode of the full-scale three-channel MPAR.
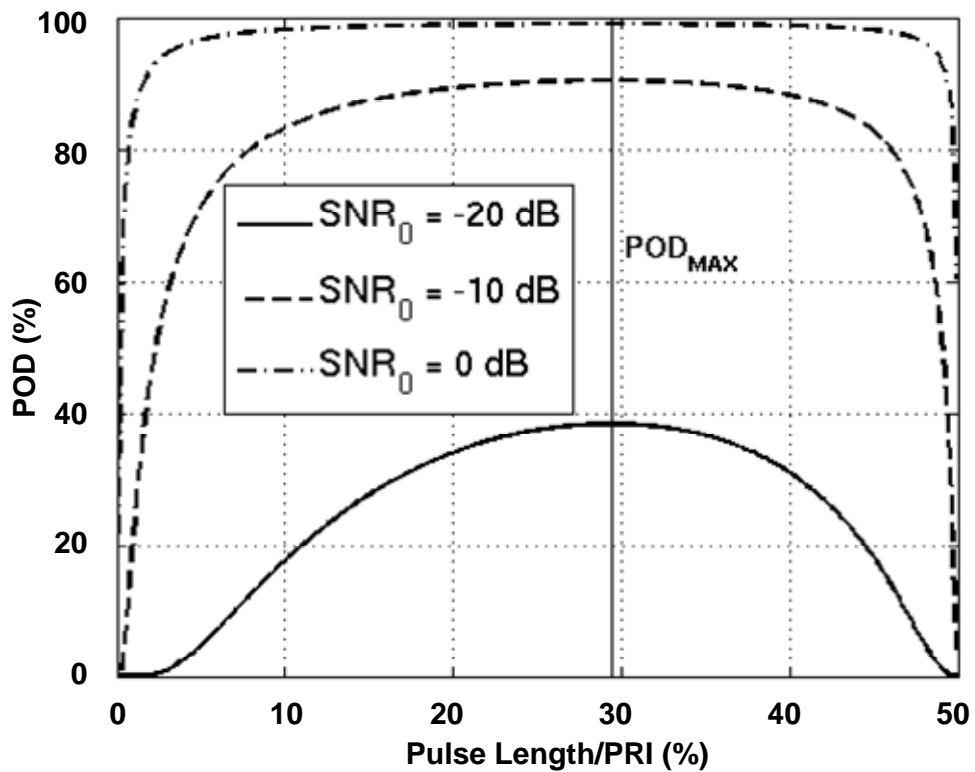
Figure 9. POD vs. pulse compression ratio for the aircraft surveillance mode of the TMPAR.

Effects of missing pulses on Doppler filtering were not included. Clearly, filters designed for a particular PRI pattern will experience performance degradation if the actual time series is different. The additional penalty for increasing pulse length would then move the POD maximum to the left in Figure 7 and Figure 9. However, since the coherent processing intervals (CPIs) for the aircraft surveillance modes are so short, it is conceivable to predefine Doppler filters for every possible PRI pattern resulting from pulse loss. There may still be some drop-off in POD performance with pulse length, but this is expected to be a minor effect.

5. WEATHER SURVEILLANCE MODE

As discussed previously, weather surveillance by radar does not result in a simple detection/no detection decision. Rather, the output consists of estimated parameter fields (reflectivity, radial velocity, and spectral width) that are characterized in quality by their deviations from the actual fields. We choose velocity for our study, because it is more sensitive to pulse loss than reflectivity and it is more important than spectral width during operational use.

Analytic equations are available for computing theoretical velocity estimate variance [5]. However, these are perturbation results that are only valid for certain limiting cases. Therefore, we decided instead to perform Monte Carlo simulations. To generate in-phase and quadrature (I&Q) baseband radar data containing the specified weather information, we employed the method outlined in [6]. Specifically, (1) a Doppler Gaussian spectrum defined by the desired weather power, velocity, and width was generated, (2) white noise was added to the level of the desired SNR, (3) each Doppler frequency bin was multiplied by the logarithm of a uniformly distributed (0 to 1) random number, and (4) an inverse DFT was performed on the resulting spectrum using random phase sampling. We used 128 frequency bins spread out across a Nyquist interval corresponding to the PRI, and generated 192 points in the time domain of which only the middle 64 were used to produce a windowing effect. Time series points corresponding to the number of pulses lost due to dead gates were then removed from random positions. Velocity was then estimated with the remaining points using the standard pulse-pair algorithm [5]. Velocity estimation error was computed as the standard deviation of the difference between the estimate and the input velocity over 1000 trials. The input velocity had a uniform random distribution within the inner half of the Nyquist interval in order to avoid aliasing errors.

We show results for the TMPAR case in Figure 10. The radar wavelength was set to 10 cm, the weather spectral width to $2 \, \mathrm{m \, s^{-1}}$, and the PRI to 1 ms. The SNR was varied as for the aircraft surveillance case. In this case, however, there is no one τ/T value that minimizes the velocity estimate error. (Results for the three-channel MPAR case were very similar (not shown).) Roughly speaking, there is no benefit to increasing the SNR above about 0 dB; the decreasing number of pulse pairs averaged only increases the parameter estimate error. In other words, increased pulse length (compression) lowers the minimum "detection" floor for weather radar, but degrades the parameter estimate quality for already-detectable signals. Fortunately there is a technique to reduce estimate variance at high SNR that can compensate for the effects of pulse compression [7]. This oversampling and whitening in range method only requires increased data transfer and computation rates.

As with the aircraft surveillance case, clutter filtering effects were not included. For the weather surveillance case, however, the CPI is generally too large to consider defining a Doppler filter for every possible PRI pattern resulting from pulse loss. We would, thus, like to examine the effects of random pulse data loss on clutter-filtered velocity estimates.
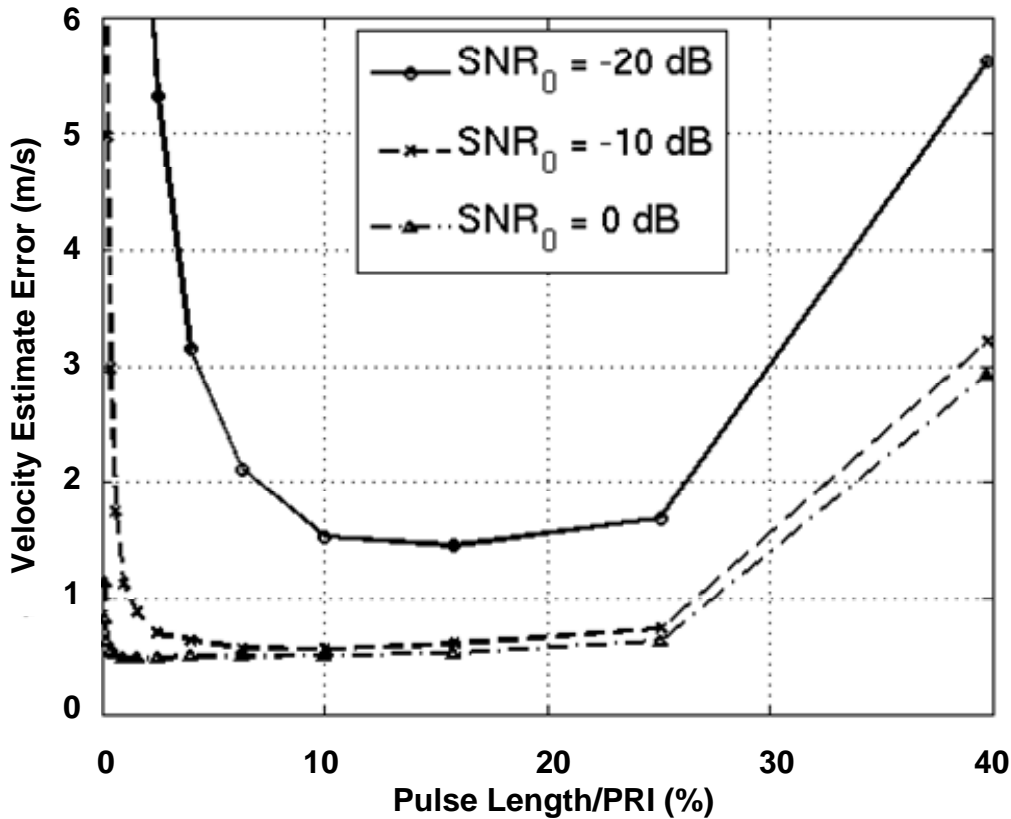
Figure 10. Velocity estimate error for the weather mode vs. pulse length normalized to PRI for the TMPAR.

We selected the Gaussian model adaptive processing (GMAP) clutter filter [8], which is being implemented in the new open radar data acquisition (ORDA) system of NEXRAD. It is also being utilized in a slightly modified form in the enhanced radar data acquisition (RDA) system of the TDWR [9]. Based on the assumed clutter spectral width and the power present in the spectrum near zero-Doppler, GMAP computes the theoretical Gaussian form of the clutter spectrum and removes the points for which this function is greater than the noise level. A Gaussian function is then generated using the computed spectral moments from the remaining points under the assumption that the clutter has been removed and only weather signals remain. The gap around zero Doppler is filled in using the spectral points of the Gaussian. The moments are recomputed and the gap refilled until there is reasonable convergence. (Clearly, it is assumed that the weather spectrum can be adequately represented by a single Gaussian.) The aim of GMAP is to reduce the clutter filter bias by filling in the stop band with spectral points that are modeled to follow the remaining weather spectrum.

For traditional mechanically scanned radars, the ground clutter spectral width is largely determined by the antenna rotation rate. An electronically scanned array (ESA) has the advantage of having a stationary beam during a dwell, and therefore the clutter spectral width is due to the motion of the target

16

itself, such as vegetation moving to the wind. We shall assume a clutter spectral width of 0.1 m s^{-1}, which is a reasonable value for wooded hills under moderate wind conditions [10]. (For ESAs, the clutter model for GMAP should perhaps be changed from Gaussian to exponential, which fits the form of wind-modulated ground clutter spectra much better [11]. We will explore this matter in the future.)

In processing the simulated I&Q time series with data gaps, we found that the spectral clutter filter performed well if the gaps were interpolated over rather than set to zero. We believe this is because ground clutter echoes inherently vary slowly with time. On the other hand, the pulse-pair estimator for velocity performed slightly better when the interpolated points were not used after the inverse DFT from the spectral clutter filter domain. This is probably because the velocity signal can fluctuate much more rapidly with time. We, therefore, followed these procedures that produced the best results.

The results for the TMPAR case are shown in Figure 11. The same weather and radar parameters were used as for Figure 10. The velocity estimation errors have generally increased compared to Figure 10, but the shapes of the curves are very similar. Thus, the previous notes and conclusions also apply to the case with clutter filter effects included. It appears that, for the weather surveillance channel, τ/T should not exceed about 10%, i.e., a pulse compression ratio of about 100. The results for the three-channel MPAR case are displayed in Figure 12. In this case, the pulse compression ratio should probably not exceed about 150.
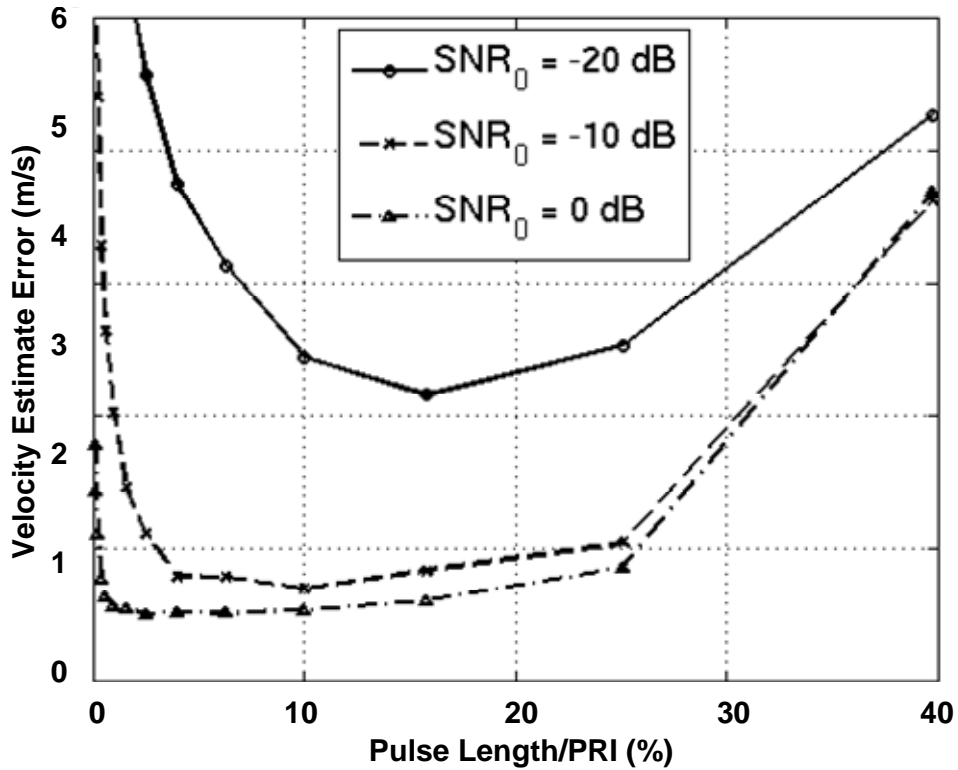
Figure 11. Velocity estimate error for the weather mode vs. pulse length normalized to PRI for the TMPAR including clutter filter effects.
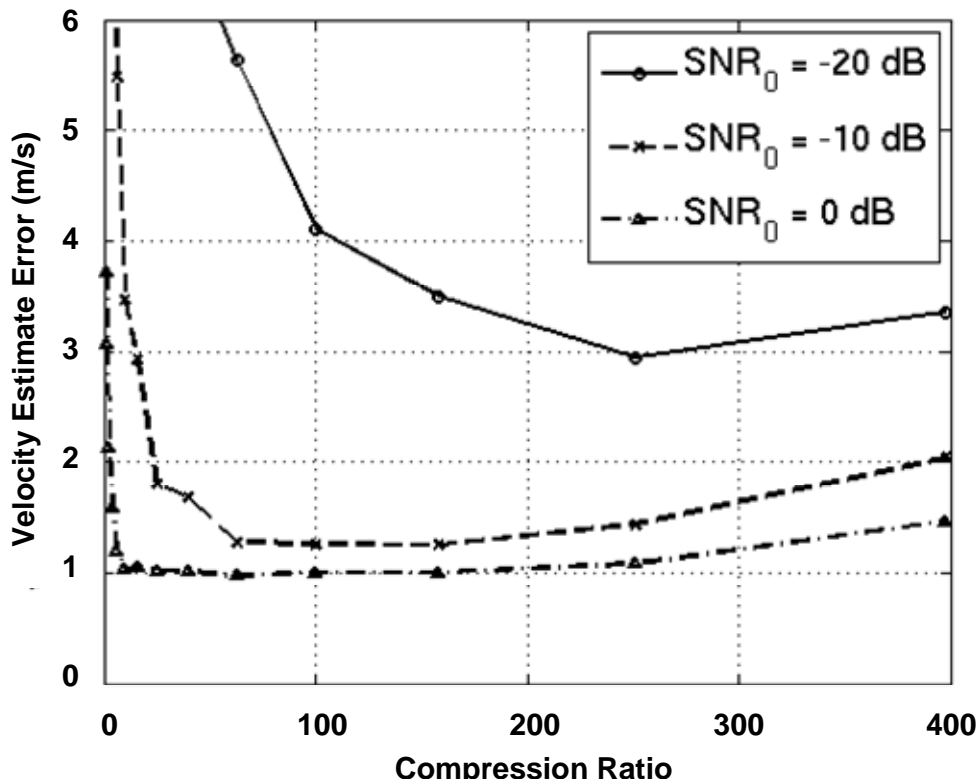

Figure 12. Velocity estimate error for the weather mode vs. compression ratio for the three-channel MPAR including clutter filter effects.

18

6. DISCUSSION

In this report we examined the limitations on pulse compression ratio (i.e., pulse length) in a multichannel radar system imposed by fill-pulse range and dead gate/pulse overlap avoidance data loss. The results are summarized in Table 1. The most severe restriction is placed by the fill-pulse range of the weather surveillance mode. This result is not so surprising, given that the sensitivity requirement for weather is more difficult to satisfy than for aircraft detection. Although the same value of C was assumed for the aircraft and weather surveillance channels requiring pulse compression in our study, it is possible to use different values of C for the two modes, e.g., the aircraft mode could have a smaller pulse compression ratio, because the sensitivity requirement is not as stringent as for the weather mode. However, "excess" sensitivity in the aircraft channels is used to speed up the volume scan rate by spoiling the beam on transmit and receiving on multiple clustered beams simultaneously [1]. Therefore, the exact degree of pulse compression to be used for each channel must be determined by using the actual radar parameters and making sure that all sensitivity and scan-time requirements can be met. The results from this report are independent of the power-aperture figures for the MPAR and TMPAR, and only give the general maximum limit on the pulse compression ratios.

TABLE 1

Maximum Recommended Pulse Compression Ratios

Radar	Mode	Maximum Pulse Compression Ratio		
		Fill-Pulse Range	Dead Gates & Pulse Overlap	Overall
MPAR	En Route A/C	620	390	130
	Weather	130	~ 150	
TMPAR	Aircraft	200	290	80
	Weather	80	~ 100	

For the MPAR, Table 1 does not include an entry for the terminal-area aircraft surveillance mode, because we assumed that no pulse compression would be used in that channel and that it would act as the fill-pulse mode. However, we see from Figure 8 that pulse data loss due to increased pulse compression in the other channels degrades the POD on this channel. To see how much the detection range is decreased, we solve for S in (10) to get the detectability factor

$$S_{\mathrm{d}}(P_{\mathrm{d}},P_{\mathrm{fa}},n,n_e) = \left[\frac{\chi_c^{-2}(1-P_{\mathrm{fa}},2n)-2(n-n_e)}{\chi_c^{-2}(1-P_{\mathrm{d}},2n)}-1\right]\frac{n_e}{n} \quad . \tag{11}$$

19

The detection range R is proportional to $S_d^{-1/4}$. We then use (9) in (11) to get S_d, with $n = n_0(1 - L)$ as before, and compute $S_d^{-1/4}$ normalized by $S_d^{-1/4}$ for $C = 1$ ($n = n_0$). The results are plotted in Figure 13, with $n_0 = 18$, $P_{fa} = 10^{-6}$, and $P_d = 0.9$. We see that the degradation in detection range for this channel with no pulse compression must be taken into account when selecting the pulse compression ratios of the other channels.
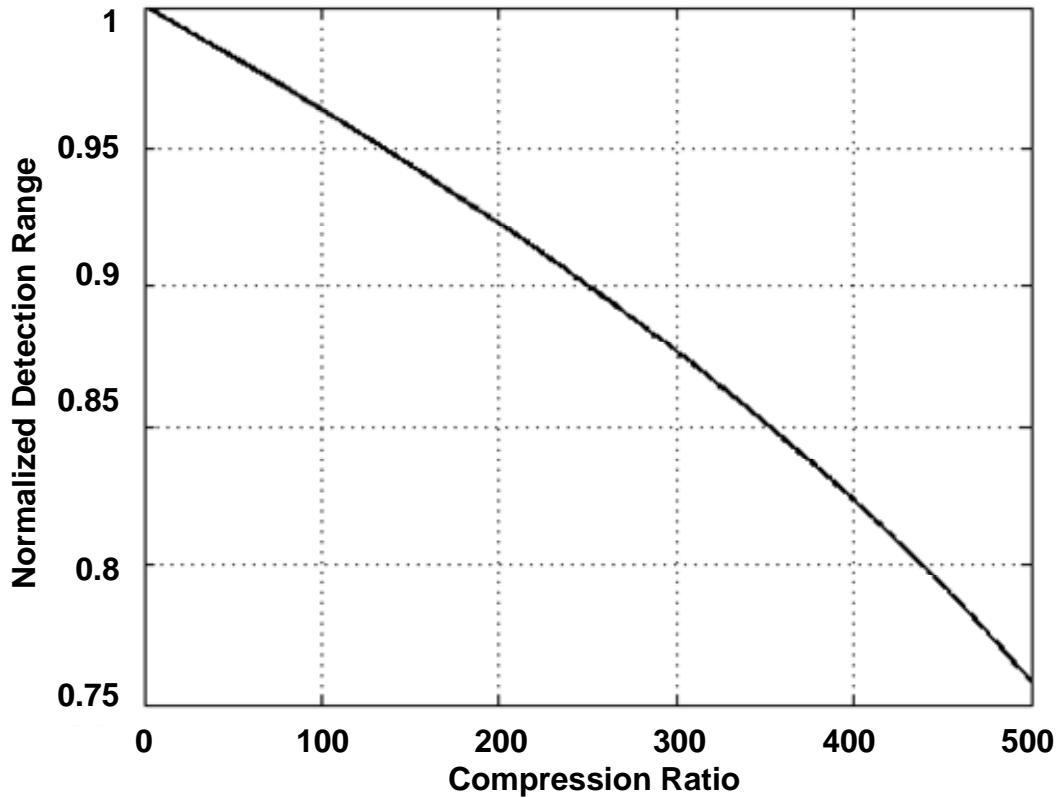

Figure 13. Normalized detection range vs. compression ratio for the terminal-area aircraft surveillance channel of the three-channel MPAR.

7. CONCLUSION

In designing a multichannel MPAR one must balance the benefits of enhanced SNR via pulse compression (lengthening) and the accompanying increase of the blind zone and loss of pulse data through dead gates and pulse overlap avoidance. In this report we quantified these effects and determined the maximum recommended pulse compression ratios for two particular configurations (three-channel MPAR and two-channel TMPAR). These results are independent of the radar peak power and antenna gain, and represent the upper bounds. Actual pulse compression ratios that would be employed are likely to be somewhat less than these values, based on fulfilling specific sensitivity and scan-time requirements with specific radar physical parameters. The results of this report will be useful for formulating those particular system specifications.

GLOSSARY

ARSR	Air Route Surveillance Radar
ASR	Airport Surveillance Radar
CPI	coherent processing interval
ESA	electronically scanned array
GMAP	Gaussian model adaptive processing
I&Q	in-phase and quadrature
MPAR	multifunction phased array radar
NEXT	Next Generation Weather Radar
POD	probability of detection
PRI	pulse repetition interval
RDA	radar data acquisition
SNR	signal-to-noise ratio
TDWR	Terminal Doppler Weather Radar
TMPAR	terminal-area multifunction phased array radar
TR	transmit/receive

REFERENCES

[1] M. Weber, J. Cho, J. Flavin, J. Herd, and M. Vai, "Multi-function phased array radar for U.S. civil-sector surveillance needs," presented at the 32nd Conf. on Radar Meteorology, Albuquerque, NM, October 24-29, 2005, Paper 12R.2. Available: http://ams.confex.com/ams/32Rad11Meso/techprogram/paper_96905.htm.

[2] J. I. Marcum, "A statistical theory of target detection by pulsed radar," *IRE Trans. Information Theory*, vol. IT-6, p. 59-268, Apr. 1960.

[3] D. K. Barton, "Universal equations for radar target detection," *IEEE Trans. Aerosp. Electron. Syst.*, vol. 41, pp. 1049-1052, July 2005.

[4] P. Swerling, "Probability of detection for fluctuating targets," *IRE Trans. Information Theory*, vol. IT-6, pp. 269-308, Apr. 1960.

[5] D. S. Zrnić, "Spectral moment estimation from correlated pulse pairs," *IEEE Trans. Aerosp. Electron. Syst.*, vol. 13, pp. 344-354, July 1977.

[6] D. S. Zrnić, "Simulation of weatherlike Doppler spectra and signals," *J. Appl. Meteor.*, vol. 14, pp. 619-620, June 1975.

[7] S. M. Torres and D. S. Zrnić, "Whitening in range to improve weather radar spectral moment estimates. Part I: formulation and simulation," *J. Atmos. Oceanic Technol.*, vol. 20, pp. 1433-1448, Nov. 2003.

[8] A. Siggia and R. E. Passarelli Jr., "Gaussian model adaptive processing (GMAP) for improved ground clutter cancellation and moment estimation," in *Proc. 3rd European Conf. on Radar in Meteorology and Hydrology*, Visby, Sweden, 2004, pp. 67-73.

[9] J. Y. N. Cho and E. S. Chornoboy, "Multi-PRI signal processing for the Terminal Doppler Weather Radar. Part I: Clutter filtering," *J. Atmos. Oceanic Technol.*, vol. 22, pp. 575-582, May 2005.

[10] H. Goldstein, "Sea echo, the origins of echo fluctuations, and the fluctuations of clutter echoes," in *Propagation of Short Radio Waves*, MIT Radiation Laboratory Series, vol. 13, D. E. Kerr, Ed. New York: McGraw-Hill, 1951, pp. 560-587.

[11] J. B. Billingsley, *Low-Angle Radar Land Clutter: Measurements and Empirical Models*. Norwich, NY: William Andrews, 2002, 722 pp.